JACC Vol. 32, No. 1
July 1998:252–60

EXPERIMENTAL STUDIES

Basis for Detection of Stenosis Using Venous Administration of Microbubbles During Myocardial Contrast Echocardiography: Bolus or Continuous Infusion?

KEVIN WEI, MD, FACC, ANANDA R. JAYAWEERA, PHD, SOROOSH FIROOZAN, MD, ANDRE LINKA, MD, DANNY M. SKYBA, PHD, SANJIV KAUL, MD, FACC

Charlottesville, Virginia

Objectives. **This study sought to determine the basis of detection of stenosis by myocardial contrast echocardiography using venous administration of microbubbles and to define the relative merits of bolus injection versus continuous infusion.**

Background. **The degree of video intensity (VI) disparity in myocardial beds supplied by stenosed and normal coronary arteries can be used to quantify stenosis severity after venous administration of microbubbles. However, the comparative merits of administering microbubbles as a bolus injection or continuous infusion has not been studied.**

Methods. **Coronary stenoses of varying severity were created in either the left anterior descending or the left circumflex coronary artery in 18 dogs. Imagent *US* (AF0150) was given as a bolus injection in 10 dogs (Group I) and as both a bolus injection and a continuous infusion in 8 dogs (Group II). For bolus injections, peak VI was derived from time–intensity plots. During continuous infusion, microbubble velocity and microvascular cross-sectional area were derived from pulsing interval versus VI plots. Myocardial blood flow (MBF) was determined using radiolabeled microspheres.**

Results. **During hyperemia, VI ratios from the stenosed versus normal beds correlated with radiolabeled microsphere–derived MBF ratios from those beds for both bolus injections ($r = 0.81$) and continuous infusion ($r = 0.79$). The basis for detection of stenosis common to both techniques was the decrease in myocardial blood volume distal to the stenosis during hyperemia. The advantage of continuous infusion over bolus injection was the abolition of posterior wall attenuation and the ability to quantify MBF.**

Conclusions. **Both bolus injection and continuous infusion provide quantitative assessment of relative stenosis severity. Compared with bolus injection, continuous infusion also allows quantification of MBF and data acquisition without attenuation of any myocardial bed.**

(J Am Coll Cardiol 1998;32:252–60)

The most frequent indication for myocardial perfusion imaging is for localizing coronary stenoses and estimate their severity (1). Myocardial contrast echocardiography (MCE) is a new method of assessing myocardial perfusion in which microbubbles are injected into the vascular system, and their presence in the myocardium is detected with ultrasound (1). Microbubbles capable of opacifying the myocardium from a venous injection have recently become available (2–5). When combined with intermittent harmonic imaging, they result in adequate myocardial opacification (2–5).

We previously showed (2) that during exogenously induced coronary hyperemia, the relative background-subtracted video intensity (VI) from different myocardial beds during a bolus intravenous injection of microbubbles reflects the relative myocardial blood flow (MBF) to these regions. We postulated (2) that the ability of VI to reflect relative MBF resulted from the closely coupled changes in MBF and myocardial blood volume (MBV) during hyperemia. More recently, we showed (6) that MBF can be quantified during a continuous intravenous infusion of microbubbles by measuring changes in mean myocardial microbubble velocity and microvascular cross-sectional area (CSA) (or MBV). The purpose of the present study was to determine the basis of detection of stenosis using venous administration of microbubbles during MCE and to compare the relative merits and drawbacks of continuous infusion versus bolus injection.

From the Cardiovascular Division, University of Virginia School of Medicine, Charlottesville, Virginia. This study was supported in part by a grant R01-HL48890 from the National Heart, Lung, and Blood Institute, National Institutes of Health, Bethesda, Maryland and by a grant from Alliance Pharmaceutical Corporation, San Diego, California. Hewlett Packard Corporation, Andover, Massachusetts provided an equipment grant, and the radiolabeled microspheres were provided by Dupont-Merck, North Billerica, Massachusetts. Dr. Wei was the recipient of a Junior Personnel Research Fellowship from the Heart and Stroke Foundation of Canada, Ottawa, Ontario, Canada, and Dr. Firoozan was the recipient of a Junior Research Fellowship from the British Heart Foundation, London, England, United Kingdom. Dr. Linka was supported by the Ciba-Geigy Jubiläums-Stiftung, Basel, Switzerland and the Theodor und Ida Herzog-Egli Stiftung, Zurich, Switzerland. Dr. Skyba is supported by a postdoctoral fellowship Grant F32-HL095410 from the National Institutes of Health. This work was presented in part at the 46th Annual Scientific Session of the American College of Cardiology, March 1997, Anaheim, California.

Manuscript received October 21, 1997; revised manuscript received March 13, 1998, accepted April 8, 1998.

Address for correspondence: Dr. Sanjiv Kaul, Cardiovascular Division, Box 158, University of Virginia Medical Center, Charlottesville, Virginia 22908. E-mail: sk@virginia.edu.

0735-1097/98/$19.00
PII S0735-1097(98)00212-5

Abbreviations and Acronyms

CBF = coronary blood flow
CBV = coronary blood volume
CSA = cross-sectional area
MBF = myocardial blood flow
MBV = myocardial blood volume
MCE = myocardial contrast echocardiography (echocardiographic)
LAD = left anterior descending coronary artery
LCx = left circumflex coronary artery
VI = video intensity
PI = pulsing interval

Methods

Animal preparation. The study protocol was approved by the animal research committee at the University of Virginia and conformed to the "Position of the American Heart Association on Research Animals Use" adopted by the Association in November 1984. A total of 18 dogs were anesthetized with 30 mg/kg^{-1} body weight of sodium pentobarbital (Abbott), intubated and ventilated with a respirator pump (model 607, Harvard Apparatus). Catheters (7F) were placed in both femoral arteries for withdrawal of reference samples during radiolabeled microsphere injections and in both femoral veins for administration of fluids, drugs and microbubbles, respectively. The tip of a 7F pulmonary artery balloon-tipped flotation catheter (model MPA-372T, Millar Instruments) was positioned in the main pulmonary artery for measurement of cardiac output.

A left lateral thoracotomy was performed, and the heart was suspended in a pericardial cradle. A 7F catheter was placed in the left atrium for pressure measurements and the injection of radiolabeled microspheres. A similar catheter was placed in the ascending aorta for the measurement of aortic pressure. Ultrasound time of flight flow probes (series SB, Transonics) were placed around the proximal portions of the left anterior descending (LAD) and left circumflex (LCx) coronary arteries and were connected to a digital flowmeter (model T206, Transonics). A 20-guage Teflon catheter (Critikon) was introduced into one of the arteries through a side branch, and a custom-designed screw occluder was placed around the vessel to produce coronary stenoses of varying severity.

Hemodynamic variables. All catheters were connected to fluid-filled pressure transducers that, like the flowmeter, were connected to a multichannel recorder (model ES 2000, Gould Electronics). Coronary blood flow (CBF) and pressures were acquired digitally at 200 Hz on an 80386-based personal computer. The signals were displayed on-line using Labtech Notebook (Laboratory Technologies). The severity of the stenosis was judged by the mean pressure gradient between the aorta and the distal coronary artery. Coronary driving pressure was calculated by subtracting the mean right atrial pressure from the mean distal coronary pressure.

MCE imaging. Imaging was performed in harmonic mode (transmit 2 MHz, receive 4 MHz) using a prototype Sonos 2500 system (Hewlett-Packard) (6). The ultrasound transducer was fixed in position with a custom-designed clamp, and a saline bath served as an acoustic interface between the transducer and the heart. The maximal dynamic range (60 dB) was used. The transmit power, focus, overall gain and image depth were held constant for each experiment.

A second-generation microbubble, Imagent *US* (AFO150, Alliance Pharmaceuticals), was used that consists of surfactant-coated microbubbles containing perfluorohexane and nitrogen (5). These microbubbles have a mean diameter of 5 μm and a mean concentration of $5 \cdot 10^{8} \cdot ml^{-1}$. For the bolus injections, a single trigger was used to acquire one end-systolic image from each cardiac cycle (2–4). For continuous infusions, dual triggering was used. The first trigger was used for microbubble destruction and the second to acquire images in end-systole (6). The interval between these triggers (pulsing interval [PI]) was increased from 150 ms to 12 s to allow progressively greater bubble replenishment of the ultrasound beam elevation (6). Up to eight end-systolic images were acquired at each PI.

MCE images were analyzed off-line, as previously described (7). For the bolus injections, end-systolic images from just before contrast injection until its disappearance from the myocardium were aligned. For continuous infusions, five images acquired at baseline and at each PI were selected and aligned. Large transmural regions of interest were defined over the LAD and LCx beds in any one image, and the VI was automatically measured from the same regions in all images.

The average VI from four to five frames before the appearance of microbubbles in the myocardium was considered to represent background. For bolus injections, time–intensity plots were generated from the background-subtracted VI and fit to a gamma-variate function: $y = Ate^{-\alpha t}$, where A

Table 1. Hemodynamic, Myocardial Blood Flow and Myocardial Contrast Echocardiographic Data From Stenosed Bed in Ten Group I Dogs

Variable	No Stenosis (n = 9)	Mild Stenosis (n = 15)	Moderate Stenosis (n = 13)	p Value
Baseline				
Mean transstenotic gradient (mm Hg)	2 ± 2	10 ± 3	23 ± 6	< 0.001
Mean CBF (ml/min)	37 ± 14	35 ± 17	34 ± 16	0.59
Peak VI*	1.3 ± 0.4	0.8 ± 0.3	0.9 ± 0.3	0.51
Hyperemia				
Mean transstenotic gradient (mm Hg)	5 ± 4†	18 ± 7†	33 ± 10†	< 0.001
Mean CBF (ml/min)	97 ± 46†	57 ± 20†	51 ± 21†	0.002
Mean MBF (ml/min per g)‡	1.9 ± 0.5	1.4 ± 0.5	1.3 ± 0.3	0.03
Peak VI*	0.9 ± 0.2†	0.7 ± 0.3	0.6 ± 0.2†	0.001

*Normalized to the nonstenosed bed. †p < 0.001 versus baseline (No Stenosis). ‡Data not obtained during baseline (No Stenosis). Data presented are mean value ± SD. CBF = coronary blood flow; MBF = myocardial blood flow; VI = video intensity.

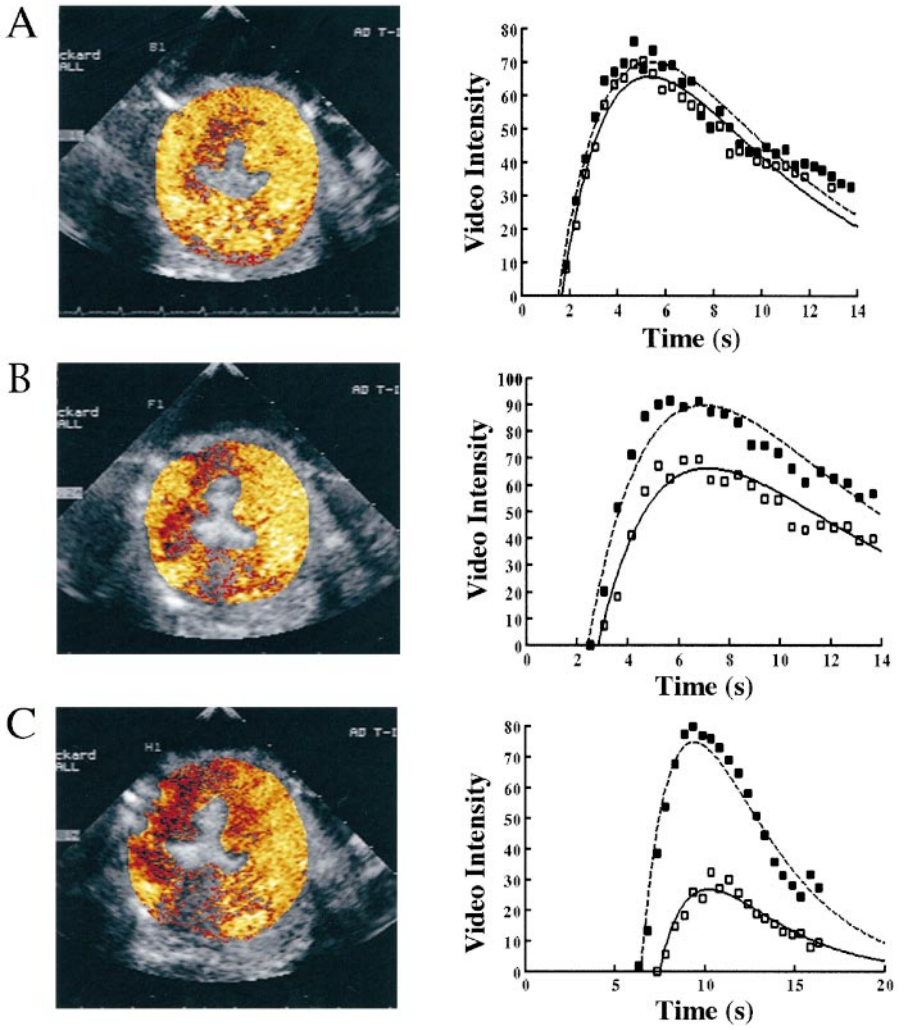

Figure 1. Color-coded images and corresponding time–intensity plots (fitted to a gamma-variate function) in a Group I dog during hyperemia. At baseline **(A),** there is no difference in VI between the LAD and LCx beds. In the presence of a mild stenosis (transstenotic pressure gradient 14 mm Hg), VI in the LAD bed decreased compared with that in the LCx bed **(B).** The decrease was even greater **(C)** in the presence of a moderate stenosis (transstenotic pressure gradient 22 mm Hg). **Open squares** = LAD bed; **solid squares** = LCx bed.

is a scaling factor; t is time; and α is proportional to the transit rate of the tracer. Peak VI was calculated from the equation A/αe (7). For continuous infusions, background-subtracted PI versus VI plots were generated and fitted to an exponential function: $y = A(1 - e^{-\beta t})$, where y is the VI at a PI t; A is the plateau VI representing microvascular CSA (or MBV); and β is the rate constant reflecting the rate of rise of VI (or the mean microbubble velocity) (6). In addition to the above analyses, color-coding was also performed to visually enhance the presence of perfusion mismatch (7). Shades of red, progressing to hues of orange, yellow and then white, represent incremental myocardial opacification. The left ventricular cavity was masked out.

Radiolabeled microsphere MBF measurement. MBF was measured using left atrial injections of $\sim 2 \cdot 10^6$ 11-μm radiolabeled microspheres (Dupont Medical Products) suspended in 4.0 ml of 0.9% saline and 0.01% Tween-80 (8). Arterial reference blood samples were collected using a constant rate withdrawal pump (model 944, Harvard Apparatus). At the end of the experiment, the short-axis slice of the left ventricle corresponding to the MCE image was cut into 16 wedge-shaped pieces, and each piece was further divided into epicardial, midcardial and endocardial segments. The tissue and blood samples were counted in a well counter with a multichannel analyzer (model 1282, LKB Wallac). Corrections were made for activity spilling from one energy window to another (8).

MBF to each epicardial, midcardial and endocardial segment was calculated from the equation $Q_m = (C_m \cdot Q_r)/Cr$, where Q_m is blood flow to the myocardial segment (ml/min); C_m is tissue count; Q_r is rate of arterial sample withdrawal (ml/min); and C_r is arterial reference sample count (8). Transmural MBF (ml/min per g) to each of the 16 wedge-shaped pieces was calculated as the quotient of the summed flows to the individual segments within that piece and their combined weight. MBF to each bed (defined by monastral blue dye injection [see later]) was then calculated by averaging the transmural MBF in the central 50% to 75% of the pieces in each bed.

Experimental protocol. In Group I dogs (n = 10), a baseline stage and up to five separate stenosis stages were performed. These stenoses were non–flow limiting at rest, and

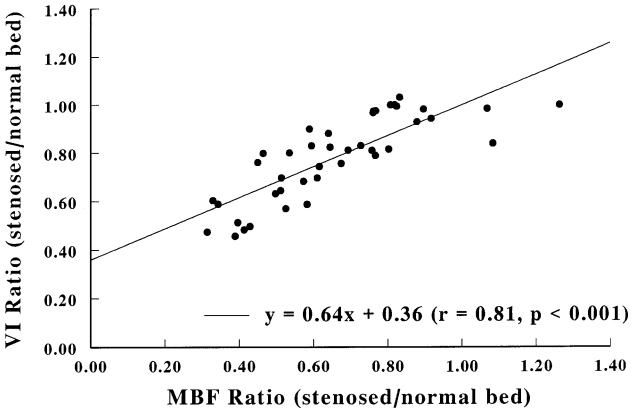

Figure 2. Relation between MBF ratio (x axis) and VI ratio (y axis) obtained from the stenosed versus the normal bed in Group I dogs during hyperemia.

their severity was defined by the pressure gradient across them. At each stage, hemodynamic data were acquired, and MCE was performed at baseline by injecting 0.2 to 0.8 ml of AFO150 (mean 0.5 ± 0.2) into the femoral vein, followed by a 5-ml 0.9% NaCl flush. The dose was determined at the beginning of each experiment and was adjusted to produce mild myocardial opacification with minimal posterior wall attenuation. It was then held constant for the duration of the study. MCE was performed after radiolabeled microspheres were injected, only during hyperemia and before and after placement of each stenosis. Hyperemia was induced by venous infusion of 0.4 μg/kg per min of WRC-0470 (Discovery Therapeutics), a selective adenosine A_{2a} receptor agonist (2,3).

In Group II dogs (n = 8), hemodynamic, radiolabeled microsphere and MCE data were obtained before and after placement of two non–flow-limiting stenoses of varying severity. All data were obtained at baseline and during hyperemia. Microbubbles were administered at each stage, both as an intravenous bolus injection and as a continuous infusion. For continuous infusions, a solution consisting of 4 ml of AFO150 in 50 ml of 0.9% saline was administered through the femoral vein at a rate of 2 ml/min, which allowed adequate myocardial opacification and no posterior wall attenuation.

At the end of the experiment, the artery undergoing stenosis was occluded at the site of the screw occluder, and monastral blue dye (Sigma Chemical) was injected into it through the distal catheter. This procedure allowed delineation of the LAD or LCx bed at the short-axis MCE imaging plane. The dog was then killed with an overdose of pentobarbital, and the heart was removed from the chest cavity. The heart was cut into five short-axis slices, and the slice corresponding to the MCE imaging plane was processed for radiolabeled microsphere analysis.

Statistical methods. Comparisons between more than two values were made using two-way repeated measures analysis of variance, and group interactions between levels of stenosis and presence or absence of hyperemia were ascertained. When analysis of variance showed significance ($p < 0.05$, two-tailed), multiple comparisons between groups was performed using a paired Student *t* test with the Bonferroni correction. Linear regression analysis (least-squares fit) was performed for deriving correlations.

Results

Group I dogs. Table 1 depicts data from the stenosed bed at baseline in the 10 Group I dogs. The severity of each stenosis was defined by the pressure gradient across it: <5 mm Hg (*none*); 5 to 14 mm Hg (*mild*); and ≥15 mm Hg (*moderate*). The epicardial CBF remained unchanged at different levels of stenosis, indicating that all stenoses were non–flow limiting at baseline. No differences were noted in the normalized background-subtracted peak VI. Table 1 also depicts data from the stenosed bed during hyperemia in Group I dogs. The mean transstenotic gradient increased, whereas the epicardial CBF and radiolabeled microsphere–derived MBF decreased with increasing levels of stenosis. These values were significantly different from baseline. The normalized peak VI was significantly lower with increasing levels of stenosis, and for moderate stenosis was significantly less than baseline values. No significant interactions were noted between stenosis severity and the presence or absence of hyperemia.

Figure 1 illustrates color-coded images and their corresponding time–intensity curves obtained before stenosis placement and in the presence of LAD stenoses of varying severity during hyperemia. In all images, some attenuation of the posterior wall is seen because of the presence of microbubbles in the left ventricular cavity. Nonetheless, much of the LCx bed

Table 2. Hemodynamic, Myocardial Blood Flow and Myocardial Contrast Echocardiographic Data From Stenosed Bed in Eight Group II Dogs

Variable	No Stenosis	Mild Stenosis	Moderate Stenosis	p Value
Baseline				
Mean transstenotic gradient (mm Hg)	2 ± 2	12 ± 3	21 ± 6	< 0.001
Mean CBF (ml/min)	39 ± 24	32 ± 21	31 ± 11	0.90
Mean MBF (ml/min per g)	1.1 ± 0.4	0.9 ± 0.3	1.0 ± 0.1	0.60
A*	1.1 ± 0.2	0.9 ± 0.3	0.9 ± 0.2	0.30
β*	1.1 ± 0.2	1.0 ± 0.2	0.9 ± 0.1	0.10
A·β*	1.2 ± 0.4	1.0 ± 0.4	0.8 ± 0.2	0.10
Hyperemia				
Mean transstenotic gradient (mm Hg)	3 ± 2	22 ± 6†	25 ± 6	< 0.001
Mean CBF (ml/min)	89 ± 48‡	47 ± 27†	38 ± 13†	0.03
Mean MBF (ml/min per g)	2.7 ± 1.3‡	1.4 ± 0.6‡	1.5 ± 0.5‡	0.03
A*	1.1 ± 0.2	0.9 ± 0.2	0.7 ± 0.3	0.005
β*	1.1 ± 0.3	0.5 ± 0.3‡	0.6 ± 0.2‡	0.001
A·β*	1.2 ± 0.3	0.4 ± 0.2‡	0.3 ± 0.1‡	< 0.001

*Normalized to nonstenotic bed. †p = 0.002, ‡p = 0.001 versus baseline (No Stenosis). Data presented are mean value ± SD. A = plateau video intensity representing microvascular cross-sectional area (or myocardial blood volume); β = rate constant reflecting rate of rise of video intensity; other abbreviations as in Table 1.

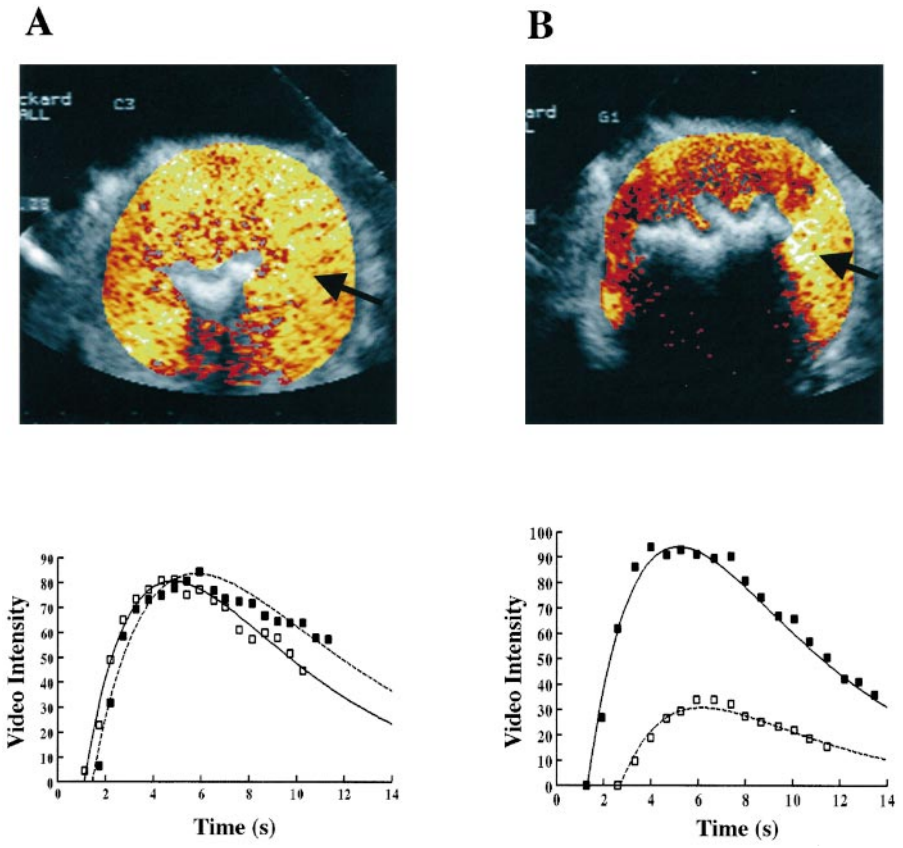

Figure 3. Color-coded images and corresponding time–intensity plots (fitted to a gamma-variate function) in a Group II dog receiving a bolus injection of contrast during hyperemia. At baseline **(A),** there is no difference in VI between the LAD and LCx beds. In the presence of a mild stenosis (pressure gradient 13 mm Hg), VI in the LAD bed is less than that in the LCx bed **(B). Arrows** indicate the region in the LCx bed from which the time–intensity curves were derived; other symbols as in Figure 1.

is visible in the lateral portion of the myocardium. Before stenosis placement, the degree of contrast enhancement (and therefore the color) is similar in the two beds. After stenoses placement, the color of the LAD bed takes on more hues of orange and red, denoting lesser degrees of contrast enhancement than that of the LCx, which still retains hues of yellow and white. Good correlation was found between the background-subtracted peak VI and the radiolabeled microsphere–derived MBF ratios from the stenosed versus normal bed during hyperemia, when data from all 10 dogs were pooled (Fig. 2).

Group II dogs. Table 2 depicts data from the stenosed bed at baseline in the eight Group II dogs; stenosis severity was classified as in the Group I dogs. No changes were noted in epicardial CBF, radiolabeled microsphere–derived MBF, background-subtracted plateau VI, mean microbubble velocity or MCE-derived MBF with increasing levels of stenosis, which, as stated earlier, were not flow limiting at rest.

Table 2 also depicts data from the stenosed bed during hyperemia in the Group II dogs. The transstenotic gradient increased significantly with increasing degrees of stenosis during hyperemia, whereas mean epicardial CBF decreased. The values for no and mild stenosis were significantly different from baseline values. Radiolabeled microsphere–derived MBF decreased progressively with increasing levels of stenosis, but was always higher than baseline values. Background-subtracted plateau VI, mean microbubble velocity and MCE-derived MBF also decreased with increasing levels of stenosis during hyperemia, and the two latter values were significantly lower than baseline values. No significant interactions were noted between the level of stenosis and the presence or absence of hyperemia.

The top panels in Figure 3 illustrate color-coded images and corresponding time–intensity curves from bolus injections during hyperemia in the absence and presence of a LAD stenosis. It is evident that peak VI in the LAD bed decreases during hyperemia in the presence of a stenosis. The top panels in Figure 4 illustrate data in the same dog during continuous infusions. Similar to Figure 3, the severity and extent of relative hypoperfusion in the stenosed bed during hyperemia are clearly seen. However, there is no posterior wall attenuation. Similar to bolus injection (Fig. 3), the VI during continuous infusion (Fig. 4) is lower during stenosis. In addition, mean microbubble velocity and MCE-derived MBF are also lower.

Figure 5A illustrates a linear relation between the MCE-derived MBF and radiolabeled microsphere–derived MBF ratios from the stenosed versus the normal bed. The relation is linear, with a slope close to the line of identity. A linear relation was also noted between the peak and plateau VI ratios from the stenosed versus normal beds during bolus injection and continuous infusion, respectively (Fig. 5B). Thus, similar information on MBV was afforded by both methods of microbubble administration.

The PI at which the greatest disparity in VI between the two

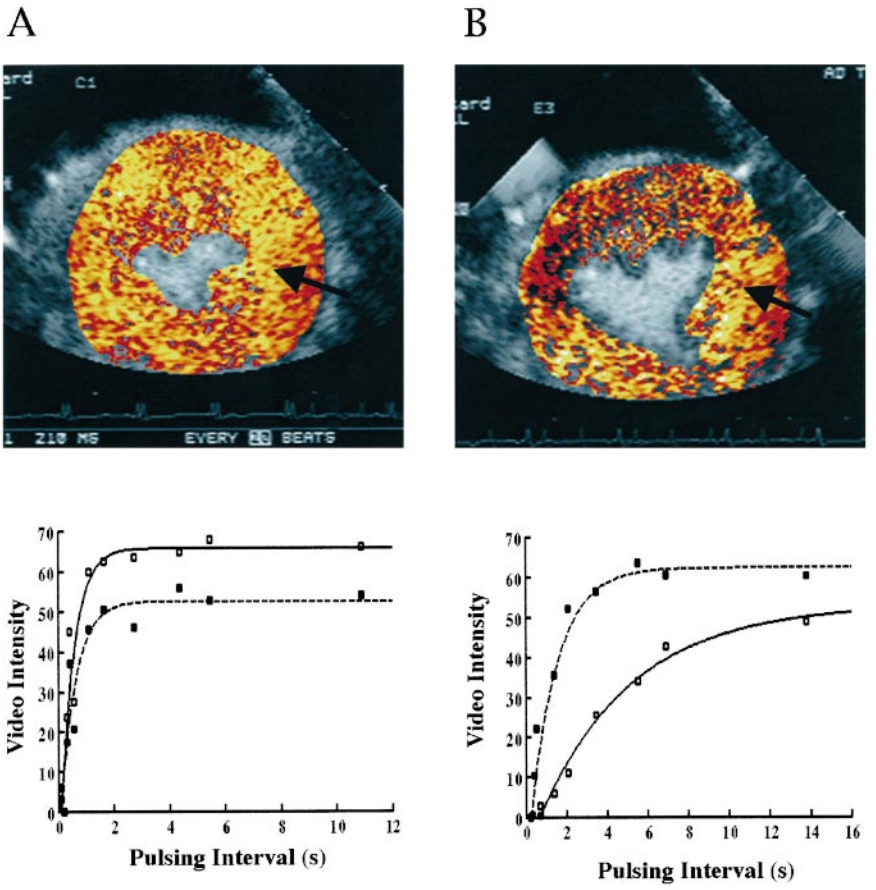

Figure 4. Color-coded images and the corresponding VI versus PI curves at baseline (**A**) and in the presence of a LAD stenosis (**B**) during continuous infusion in the same Group II dog as in Figure 3. The images correspond to the point in the curves where maximal contrast disparity between the stenosed and normal beds was seen. Symbols as in Figure 3.

beds is seen during continuous infusions can also be selected from the PI versus VI plots (Fig. 6). Panels A to C in Figure 6 depict three contrast-enhanced color-coded images obtained at different PIs during continuous infusion in a dog with a very mild stenosis. Panel D in the same image illustrates the PI at which these images were selected. Only in panel B is the VI disparity most clearly seen. This image can be selected from the sequence of images to optimize the display of both the severity of stenosis and the extent of relative hypoperfusion.

Hemodynamic results. No effects were noted on left atrial, right atrial and aortic pressures or on cardiac output during repeated injections of AFO150 in Group I and II dogs (total dose ~20 and 35 ml, respectively) (Table 3).

Discussion

Basis for detection of stenosis during venous administration of microbubbles. The entire coronary system (epicardial conduit arteries, arterioles, capillaries, venules and veins) contains ~12 ml of blood/100 g of left ventricular mass (total CBV), one-third of which is in the capillaries (9). The blood present in the left ventricular myocardial vessels is the MBV and measures ~4.5 ml/100 g. When a mild to moderate stenosis (<85% lumen diameter narrowing) is present on an epicardial coronary artery, baseline MBF is maintained at normal levels by vasodilation of arterioles distal to the stenosis

Figure 5. A, Relation between radiolabeled microsphere-derived MBF ratio (x axis) and MCE-derived MBF (A·B ratio) from the stenosed versus normal bed in all Group II dogs during hyperemia (y axis). **B,** Relation between peak VI ratio during bolus injection (x axis) and plateau VI ratio during continuous infusion (y axis) from the stenosed versus normal bed in all Group II dogs.

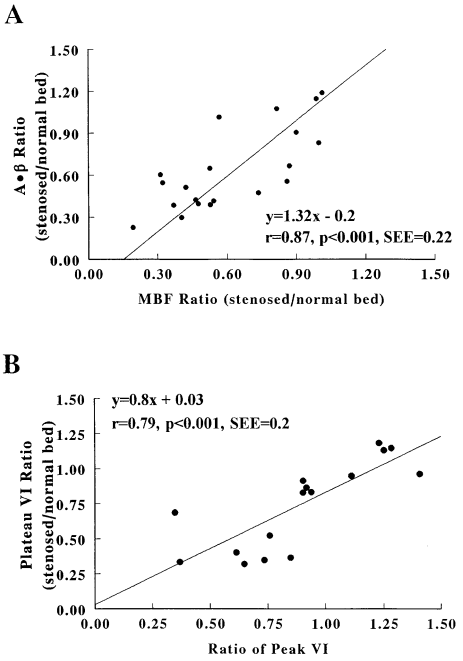

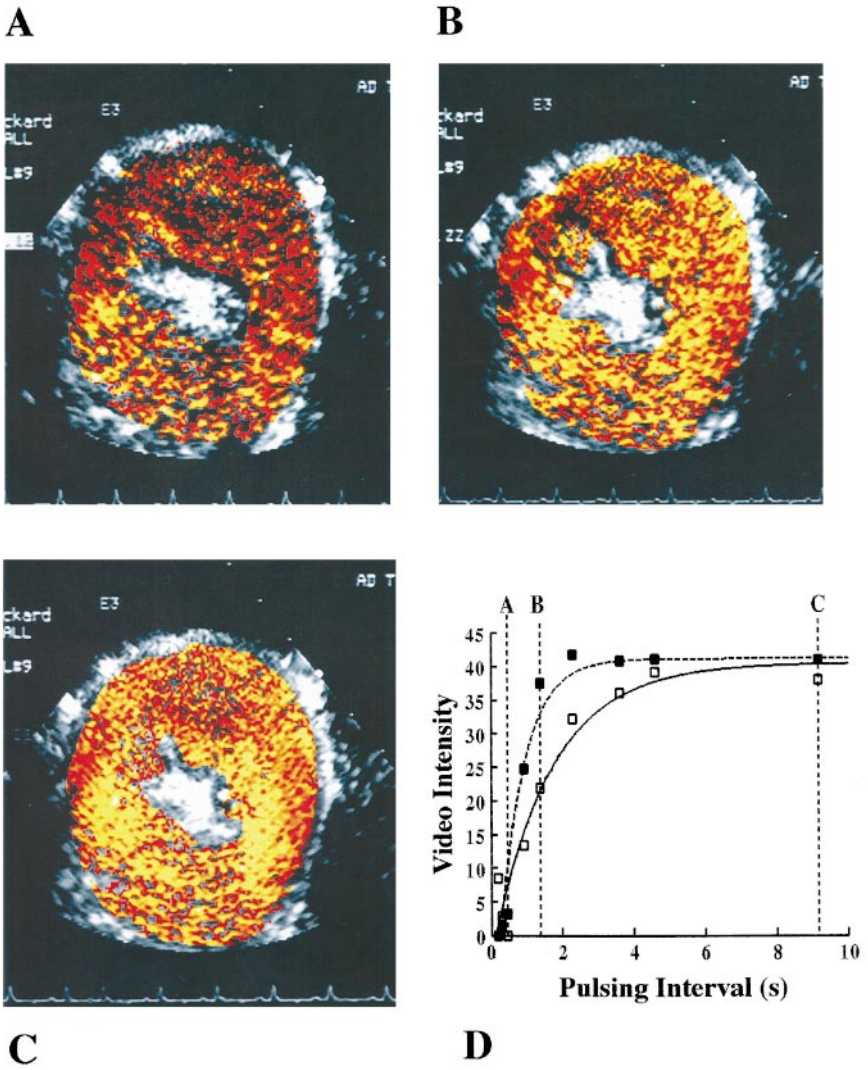

Figure 6. Color-coded images during continuous infusion in a Group II dog (**A to C**) with a mild stenosis at three different PIs. The image showing the maximal VI difference between the stenosed (LAD) and normal (LCx) beds (**B**) was selected from the VI versus PI curve (**D**). This image best represents the presence and severity of stenosis. Symbols as in Figure 1.

(10). The magnitude of this response is related to the severity of stenosis. It follows, therefore, that the measurement of CBV at rest can provide an estimate of stenosis severity. We and others have previously shown that CBV increases with increasing levels of stenosis (11,12). These results were obtained from the measurement of mean transit rates after direct bolus injections of microbubbles into the coronary artery, which reflect changes in the entire CBV (13).

In the present study, we did not observe any change in myocardial VI at baseline despite the placement of mild to moderate stenoses, which indicates that in the presence of non–flow-limiting stenoses at rest, MBV remains constant despite increases in total CBV. This phenomenon occurs because autoregulation does not principally involve the vessels within the myocardium, the majority of which (>90%) are capillaries (9). In comparison to the situation at rest, a decrease in MBV was noted for increasing levels of stenosis during hyperemia.

Based on our experience with bolus injections, we previously postulated that MBV may actually decrease distal to the stenosis during hyperemia (2,14). However, with bolus injections we could not determine whether the lower VI in the stenosed bed was actually due to an absolute decrease in MBV distal to the stenosis or simply relative to a greater MBV increase in the normal bed. In the present study, since the concentration of microbubbles in the blood remained constant during continuous infusions, a decline in myocardial VI distal to a stenosis indicates an actual decline in MBV. The mechanism for the decrease in MBV is not known but indicates a reduction in capillary density distal to the stenosis in the presence of hyperemia. This finding forms the basis for the detection and determination of the physiologic relevance of a coronary stenosis with MCE, irrespective of the method of contrast injection.

Bolus or continuous infusion? To produce myocardial opacification from a venous injection, we previously (2,3) used large doses of microbubbles, which resulted in severe attenuation of the posterior half of the heart. It was therefore necessary to wait for the microbubble concentration in the left ventricular cavity to decrease before VI measurements in the

Table 3. Hemodynamic Effects of AFO150 in Group I and II Dogs*

	RAP (mm Hg)	LAP (mm Hg)	AoP (mm Hg)	CO (liters/min)
Group I (n = 10)				
Baseline	8 ± 6	12 ± 3	87 ± 12	3 ± 1
Injection 1	8 ± 4	15 ± 4	86 ± 9	3 ± 1
Injection 2	8 ± 5	15 ± 2	77 ± 7	3 ± 1
Injection 3	7 ± 3	15 ± 5	79 ± 10	4 ± 1
Injection 4	8 ± 2	16 ± 3	77 ± 8	3 ± 1
Group II (n = 8)				
Baseline	7 ± 1	13 ± 3	102 ± 12	—
Infusion 1	7 ± 1	14 ± 3	96 ± 10	—
Infusion 2	7 ± 1	13 ± 2	90 ± 16	—

*No interstage differences noted. Data presented are mean value ± SD. AoP = mean aortic pressure; CO = cardiac output; LAP = left atrial pressure; RAP = right atrial pressure.

LAD or LCx beds could be made (2,3). Consequently, our measurements were not necessarily performed when maximal VI disparity was noted between the two beds. In the present study, we adjusted our doses for bolus injections to levels where adequate myocardial opacification could be produced with minimal posterior wall attenuation. As can be appreciated from Figures 1 and 3, myocardial VI measurements could be made simultaneously from both beds during peak contrast effect, despite the presence of posterior wall attenuation.

The difference between bolus and continuous infusion is that in the former, the concentration of microbubbles in blood changes with time, whereas in the latter, it remains stable after equilibration is reached. In either case, the relative VI between two myocardial beds reflects the relative MBV fractions of those beds (2), provided that the microbubble concentration is low enough to be in the linear range of its relation with VI (15). The obvious advantage of bolus injection is that it can be performed in a rapid manner and can provide an immediate qualitative assessment of stenosis severity during hyperemia. However, we believe that continuous infusion is a better approach for detection of stenosis for several reasons:

1. During continuous infusion, the dose of microbubbles can be customized to individual patients. There is great variability in the degree of tissue attenuation in different patients, and an individualized dose is more appropriate to provide meaningful results.

2. Posterior wall attenuation can be largely abolished with continuous infusions by titrating the rate of infusion, something almost impossible to achieve consistently with a bolus injection. Shadowing of the posterior wall has so far precluded the use of parasternal views during bolus injections. These views are important for the comprehensive evaluation of patients with coronary artery disease.

3. A constant infusion provides the time and leisure to interrogate each myocardial segment in detail, using even unorthodox views, without having to worry about missing a segment because of the limited duration of myocardial opacification afforded by a bolus injection.

4. The same person (sonographer or physician) can start the infusion, adjust the rate of administration and perform the entire examination. Another person is not required for repeated microbubble administration, as is needed with bolus injections.

5. Both microbubble velocity and MBV can be assessed with this approach. If myocardial VI can be calibrated to left ventricular VI, and if the beam elevation is known, then the product of microbubble velocity and MBV can provide a quantitative assessment of MBF (6).

Conclusions. In the present study, we evaluated two approaches for detection of coronary stenosis from venous administration of microbubbles: bolus injection and continuous infusion. We determined that the basis for detection of stenosis during hyperemia common to both methods is a decrease in MBV. We also discussed the merits and potential disadvantages of both approaches. Studies in patients need to be performed to determine which approach is most suitable in the clinical setting.

We are grateful to Norman C. Goodman, BS for technical assistance and to Robert D. Abbott, PhD for advice regarding statistical methods.

References

1. Lindner JR, Kaul S. Myocardial perfusion imaging using tracers other than radioisotopes and detectors other than gamma cameras. In: Beller GA, Zaret BL, editors. Nuclear Cardiology: State-of-the-art and Future Directions. 2nd ed. Mosby Year Book. In press.
2. Firschke C, Lindner JR, Wei K, Skyba D, Goodman NC, Kaul S. Myocardial perfusion imaging in the setting of coronary artery stenosis and acute myocardial infarction using venous injection of FS-069, a second generation echocardiographic contrast agent. Circulation 1997;96:959–67.
3. Lindner JR, Firschke C, Wei K, Goodman NC, Skyba DM, Kaul S. Myocardial perfusion characteristics and hemodynamic profile of MRX-115, a venous echocardiographic contrast agent, during acute myocardial infarction. J Am Soc Echocardiogr 1998;11:36–46.
4. Porter TR, Xie F. Transient myocardial contrast after initial exposure to diagnostic ultrasound pressures with minute doses of intravenously injected microbubbles: Demonstration and potential mechanisms. Circulation 1995; 92:2391–5.
5. Mulvaugh SL, Foley DA, Aeschbacher BC, Klarich KK, Seward JB. Second harmonic imaging of an intravenously administered echocardiographic contrast agent. Visualization of coronary arteries and measurement of coronary blood flow reserve. J Am Coll Cardiol 1996;27:1519–25.
6. Wei K, Firoozan S, Jayaweera AR, Linka A, Skyba DM, Kaul S. Quantification of myocardial blood flow with ultrasound-induced destruction of microbubbles administered as a continuous infusion. Circulation 1998;97: 473–83.
7. Jayaweera AR, Sklenar J, Kaul S. Quantification of images obtained during myocardial contrast echocardiography. Echocardiography 1994;11:385–96.
8. Heyman MA, Payne BD, Hoffman JI, Rudolf AM. Blood flow measurements with radionuclide-labeled particles. Prog Cardiovasc Dis 1977;20:52–79.
9. Kassab GS, Lin DH, Fung YB. Morphometry of pig coronary venous system. Am J Physiol 1994;267:H2100–13.
10. Gould KL, Lipscomb K. Effects on coronary stenoses on coronary flow reserve and resistance. Am J Cardiol 1974;34:48–55.
11. Lindner JR, Skyba DM, Goodman NC, Jayaweera AR, Kaul S. Changes in myocardial blood volume with graded coronary stenosis: an experimental evaluation using myocardial contrast echocardiography. Am J Physiol 1007; 272:H567–75.

12. Wu CC, Feldman MD, Mills JD, Fisher D, Jafar MZ, Villanueva FS. Myocardial contrast echocardiography can be used to quantify intramyocardial blood volume: new insights into structural mechanisms of coronary autoregulation. Circulation 1997;96:1004–11.
13. Kaul S, Jayaweera AR. Coronary and myocardial blood volumes: noninvasive tools to assess the coronary microcirculation? Circulation 1997;96:719–24.
14. Ismail S, Jayaweera AR, Camarano G, Gimple LW, Powers ER, Kaul S. Relation between air-filled albumin microbubble and red blood cell rheology in the human myocardium: influence of echocardiographic systems and chest wall attenuation. Circulation 1996;94:445–51.
15. Jayaweera AR, Ismail S, Kaul S. Attenuation deforms time-intensity curves during contrast echocardiography: implications for the assessment of transit rates. J Am Soc Echocardiogr 1994;7:590–7.